Electronic Supplementary Information (ESI)

Highly selective CO_2 capture of an *agw*-type metal-organic framework with inserted amides: experimental and theoretical studies

Jingui Duan[a], Zhen Yang[b], Junfeng Bai*[a], Baishu Zheng[a], Yizhi Li[a], Shuhua Li*[b]

[a]State Key Laboratory of Coordination Chemistry School of Chemistry and Chemical Engineering Nanjing University, Nanjing 210093 (P.R. China) E-mail: bjunfeng@nju.edu.cn

[b]Institute of Theoretical and Computational Chemistry, Nanjing University, Nanjing 210093 (P.R. China) E-mail: shuhua@nju.edu.cn

General information

All the reagents and solvents were commercially available and used as received. The elemental analysis was carried out with a Perkin-Elmer 240C elemental analyzer. The FTIR spectra were recorded from KBr pellets in the range of 4000-400 cm-1 on a VECTOR 22 spectrometer. Thermal analyses were performed on a Universal V3.9A TA Instruments from room temperature to 600°C with a heating rate of 10°C/min under flowing nitrogen. 1H NMR spectra were recorded on a Bruker DRX-500 spectrometer at ambient temperature with tetramethylsilane as an internal reference. The powder X-ray diffraction patterns (PXRD) measurements were carried on a Bruker axs D8 Advance 40kV, 40mA for CuKα (λ= 1.5418 Å) with a scan rate of 0.2 s/deg at room temperature.

Synthesis of H_3L

The ligand H_3L (5-(4-Carboxy-benzoylamino)-isophthalic acid) was synthesized from 4-Chlorocarbonyl-benzoic acid and 5-Amino-isophthalic acid according to a method reported by Cavalleri et al[1]. Anal. Calcd. $C_{16}H_{11}NO_7$: C, 58.36; H, 3.37; N, 4.25%.Found: C, 58.21; H, 3.22; N, 4.59%. m.p.: >330□. IR(KBr, pellet, cm^{-1}): 3324(s), 1697 (s), 1655 (s), 1608 (s), 1558 (s), 1417(s) 1285(s), 1112(s), 914(s), 875(s), 760(s), 665(s), 603(s). ^1H NMR (400 MHz, C_2D_6OS): d = 8.05 (m, 1H), 8.10 (m, 4H), 8.23 (m, 1H), 8.68 (m, 2H).

Synthesis of NJU-Bai3

A mixture of $CuCl_2 \cdot 2H_2O$ (30mg, 0.18mmol), H_3L (20mg, 0.06mmol), HNO_3 (10μl, 16mol/L) and N,N-dimethylacetamide (DMA)/methanol/H_2O = 3:3:0.5(2 ml) was stirred for ca. 10 min in air then transferred and sealed in a 20 ml Teflon-lined autoclave, which was heated at 75°C for 24h and then 85°C for 48h. After cooling to the room temperature, the blue block crystals were obtained. Yield: 53% (based on H_3L). Anal. Calcd for evacuated samples of NJU-Bai3 ($C_{32}H_{22}Cu_3N_2O_{17}$): C, 42.84; H, 2.47; N, 3.12; Found: C, 42.82; H, 2.29; N, 3.16. IR (KBr, pellet, cm-1): 3402 (s), 1656 (s), 1556(m), 1373 (s), 1279 (s), 1254 (s), 1147 (s), 1102 (s), 1061 (s), 1016(s), 843 (s), 730 (s), 549 (s).

Single crystal X-ray study

Single-crystal X-ray diffraction data were measured on a Bruker Smart Apex CCD diffractometer at 293 K using graphite monochromated Mo/Kα radiation (λ = 0.71073 Å). Data reduction was made with the Bruker Saint program. The crystal of NJU-Bai3 was mounted in a flame sealed capillary containing a small amount of mother liquor to prevent desolvation during data collection, and data were collected at 298K. The structures were solved by direct methods and refined with full-matrix least squares technique using the SHELXTL package [2]. Non-hydrogen atoms were refined with anisotropic displacement parameters during the final cycles. Organic hydrogen atoms were placed in calculated positions with isotropic displacement parameters set to 1.2×Ueq of the attached atom. The hydrogen atoms of the ligand and water molecules could not be located, but are included in the formula. The unit cell includes a large region of disordered solvent molecules, which could not be modeled as discrete atomic sites. We employed PLATON/SQUEEZE [3] to calculate the diffraction contribution of the solvent molecules and, thereby, to produce a set of solvent-free diffraction intensities; structures were then refined again using the data generated.

Sample activation

The solvent-exchanged sample (200 mg) was prepared by immersing the as-synthesized samples in acetone for 3 days to remove the nonvolatile solvates, and the extract was decanted every 8 hours and fresh acetone was replaced. The completely activated sample was obtained by heating the solvent-exchanged sample at 130 °C under a dynamic high vacuum for 48 hours. During this time, the pale blue sample changed to a deep purple-blue color indicative of the presence of unsaturated metal Cu^{II} sites (Fig S4). The similar color change upon activation was observed for other frameworks that constructed from copper paddlewheel clusters [4]. The completely-activated samples were moisture sensitive and a few minutes of exposure to air could change the sample's color back to pale blue.

Adsorption experiments

In the gas sorption measurement, Ultra-high-purity grade, N_2, CH_4 (>99.999%) and CO_2 gases (99.995% purity) were used throughout the adsorption experiments. All of the measured sorption isotherms have been repeated several times to confirm the reproducibility within

experimental error. Low-pressure N_2, CO_2, CH_4 and H_2 adsorption measurements (up to 1 bar) were performed on Micromeritics ASAP 2020 M+C surface area analyzer. Helium was used for the estimation of the dead volume, assuming that it is not adsorbed at any of the studied temperatures. To provide high accuracy and precision in determining P/P_0, the saturation pressure P_0 was measured throughout the N_2 analyses by means of a dedicated saturation pressure transducer, which allowed us to monitor the vapor pressure for each data point. A part of the N_2 sorption isotherm in the P/P_0 range 0.01-0.08 was fitted to the BET equation to estimate the BET surface area and the Langmuir surface area calculation was performed using all data points. The pore size distribution was obtained from the DFT method in the Micromeritics ASAP2020 software package based on the N_2 sorption at 77K.

High pressure gravimetric gas sorption measurements

High pressure adsorption of CO_2, N_2 and CH_4 were measured using an IGA-003 gravimetric adsorption instrument (Hiden-Isochema, UK) over a pressure range of 0-20 bar at 273 and 298 K, respectively. Before measurements, about 120 mg solvent-exchanged samples were loaded into the sample basket within the adsorption instrument and then degassed under high vacuum at 130 °C for 20 h to obtain about 65 mg fully desolvated samples. At each pressure, the sample mass was monitored until equilibrium was reached (within 25 minutes).

Estimation of the isosteric heats of gas adsorption

A virial-type[5] expression comprising the temperature-independent parameters a_i and b_i was employed to calculate the enthalpies of adsorption for CH_4 and CO_2 (at 273, 293 and 298 K) on NJU-Bai3. In each case, the data were fitted using the equation:

$$\ln P = \ln N + 1/T \sum_{i=0}^{m} a_i N^i + \sum_{i=0}^{n} b_i N^i \quad (1)$$

Here, P is the pressure expressed in Torr, N is the amount adsorbed in mmol/g, T is the temperature in K, a_i and b_i are virial coefficients, and m, n represent the number of coefficients required to adequately describe the isotherms (m and n were gradually increased until the contribution of extra added a and b coefficients was deemed to be statistically insignificant towards the overall fit, and the average value of the squared deviations from the experimental

values was minimized).

$$Q_{st} = -R\sum_{i=0}^{m} a_i N^i \quad (2)$$

Here, Q_{st} is the coverage-dependent isosteric heat of adsorption and R is the universal gas constant.

Binary mixture adsorption

IAST was used to predict binary mixture adsorption from the experimental pure-gas isotherms. In order to perform the integrations required by IAST, the single-component isotherms should be fitted by a proper model. There is no restriction on the choice of the model to fit the adsorption isotherm, but data over the pressure range under study should be fitted very precisely[6]. Several isotherm models were tested to fit the experimental pure isotherms for CO_2, N_2 and CH_4 in NJU-Bai3, and the dual-site Langmuir-Freundlich equation was found to best fit the experimental data:

$$q = q_{m1} \cdot \frac{b_1 \cdot P^{1/n_1}}{1 + b_1 \cdot P^{1/n_1}} + q_{m2} \cdot \frac{b_2 \cdot P^{1/n_2}}{1 + b_2 \cdot P^{1/n_2}} \quad (3)$$

Here, P is the pressure of the bulk gas at equilibrium with the adsorbed phase (kPa), q is the adsorbed amount per mass of adsorbent (mol/kg), q_{m1} and q_{m2} are the saturation capacities of sites 1 and 2 (mol/kg), b_1 and b_2 are the affinity coefficients of sites 1 and 2 (1/kPa), and n_1 and n_2 represent the deviations from an ideal homogeneous surface. Fig. 6 shows that the dual-site Langmuir-Freundlich equation fits the single-component isotherms extremely well. The R_2 values for all the fitted isotherms were over 0.99997. Hence, the fitted isotherm parameters were applied to perform the necessary integrations in IAST.

Computational methods

To characterize the adsorption sites of CO_2 molecules in NJU-Bai3, grand canonical Monte Carlo (GCMC) simulations and first-principles calculations were carried out here.

Potential model used in GCMC simulation

To eliminate the complexity in the simulations, the NJU-Bai3 framework was fixed at the

crystallographic data based on the Single-crystal X-ray diffraction. Four unit cells of NJU-Bai3 (2 × 2 × 1) were used to construct the simulation box of the GCMC run. Then, the structural parameters of simulation box are a = b = 37.402 Å and c = 49.754 Å, as well as α = β = 90 degrees and γ = 120 degrees.

The non-bonded interactions between the CO_2 molecules and NJU-Bai3 were described by both the Coulomb and Lennard-Jones (LJ) interactions. A rigid three-site EPM2 model[7] with partial charge on each atom was used for CO_2 molecules, since this model can accurately reproduce the experimental critical point and liquid–vapor coexistence curve of CO_2 molecules. For NJU-Bai3, all LJ parameters were taken from the Universal force field (UFF)[8] except for the Cu atom[9]. The mixing LJ parameters between different atomic types were calculated by the Lorentz-Berthelot mixing rule. All LJ parameters used in this work are given in Table S1.

Table S1. LJ parameters for all atomic types used in GCMC simulations

Atomic type	σ (Å)	ε (kcal/mol)
C (CO_2)	2.757	0.056
O (CO_2)	3.033	0.160
H (MOF)	2.646	0.044
C (MOF)	3.531	0.105
N (MOF)	3.356	0.069
O (MOF)	3.209	0.060
Cu (MOF)	1.841	0.043

Since the original UFF does not include the Coulomb interaction between atoms, we have obtained partial atomic charges on all atoms in the NJU-Bai3 by performing ab initio calculations on some small cluster models due to the large size of NJU-Bai3 as adopted in the previous work [10]. As shown in Fig. S1, we constructed three small cluster models from the NJU-Bai3, which are denoted as Cluster **A**, **B**, and **C**, respectively. The part atomic charges obtained from first-principles calculations are only adopted in the green frame of each cluster model (see Fig. S1). To determine the ground-state spins of the three Cluster **A**, **B** and **C**, single-point energy calculations are performed at different spin states at the unrestricted B3LYP/6-31g** level. Then, the atomic charges are chosen from the lowest-energy spin with the Merz-Singh-Kollman (MK) scheme[11], where atomic charges are fitted to reproduce the electrostatic potential at number of points. To keep the neutral feature of NJU-Bai3, the positive and negative charges are scaled slightly (< 5%). With this strategy, the obtained partial atomic charges for all atomic types in NJU-Bai3 are given in the Table S2.

Table S2. The partial atomic charges used of NJU-Bai3 in this work.

Atomic type	Cu1	Cu2	O1	O2	O3	O4
Charge (e)	1.050	0.958	-0.613	-0.528	-0.530	-0.530
Atomic type	N1	C1	C2	C3	C4	C5
Charge (e)	-0.811	0.689	0.042	-0.151	-0.100	-0.148
Atomic type	C6	C7	C8	C9	C10	C11
Charge (e)	0.757	0.498	-0.306	0.050	-0.167	0.486
Atomic type	H1X	H3	H4	H8	H10	
Charge (e)	0.395	0.153	0.137	0.196	0.210	

GCMC simulation details

Before running GCMC simulations, NPT molecular dynamics (MD) simulations were first performed for bulk CO_2 at the pressure of 1 atm with the temperatures of 273 K and 298 K, respectively. 128 CO_2 molecules were included in the simulation box. The Nosé–Hoover method was applied for maintaining the constant temperature with the periodic boundary conditions in all three directions. The Newton's equations of motion were integrated by using the velocity Verlet algorithm with a time step of 2 fs. At each MD run, the simulation time was typically 5 ns for equilibration, and then the next 5 ns for the production stage. Then on the basis of the equilibration configurations from the MD simulations, the corresponding chemical potentials of bulk CO_2 were determined by the test-particle method proposed by Widom[12].

It is well-known that the chemical potentials of the adsorbate in the adsorbed and bulk phases are equivalent at the thermodynamic adsorption equilibrium. Therefore, GCMC simulations were carried out for the adsorption of CO_2 in NJU-Bai3 with input of above chemical potentials at 273 K and 298 K, respectively. Four basic types of trial moves with equal probabilities were included in the simulation: translation, rotation, insertion, and deletion. The acceptance rate in the translation and rotation steps were controlled about 50% by adjusting the maximum magnitudes of translation and rotation, respectively. For increasing the acceptance efficiency of insertion, the configuration-biased method [13] was used for the insertion step. The cutoff distance for the LJ interaction was 14.0 Å and the electrostatic interactions were calculated using the Particle Mesh

Ewald method [14] with a real-space cutoff of 14.0 Å and a tolerance of 10^{-5}. Each GCMC simulation was totally run for 4×10^6 trial moves. The first 1×10^6 moves were used for the equilibration and the subsequent 3×10^6 moves were used for ensemble averages.

First-principles calculation

To further analyze the binding energies between the NJU-Bai3 and CO_2 molecule at different adsorption sites, a series of first-principles calculations were performed for the complex of CO_2 molecule and each cluster model extracted from NJU-Bai3. All geometry optimizations were performed at the B3LYP/6-31G** level. Based on the optimized geometries, the binding energy were calculated with the correction of basis set superposition error (BSSE) at the B3LYP/6-311++G** level. All first-principles calculations in this work were performed with the Gaussian 03 program. The binding energy is expressed as

$$E_{binding} = E(CO_2 / cluster) - E(cluster) - E(CO_2) + E_{BSSE} \quad (4)$$

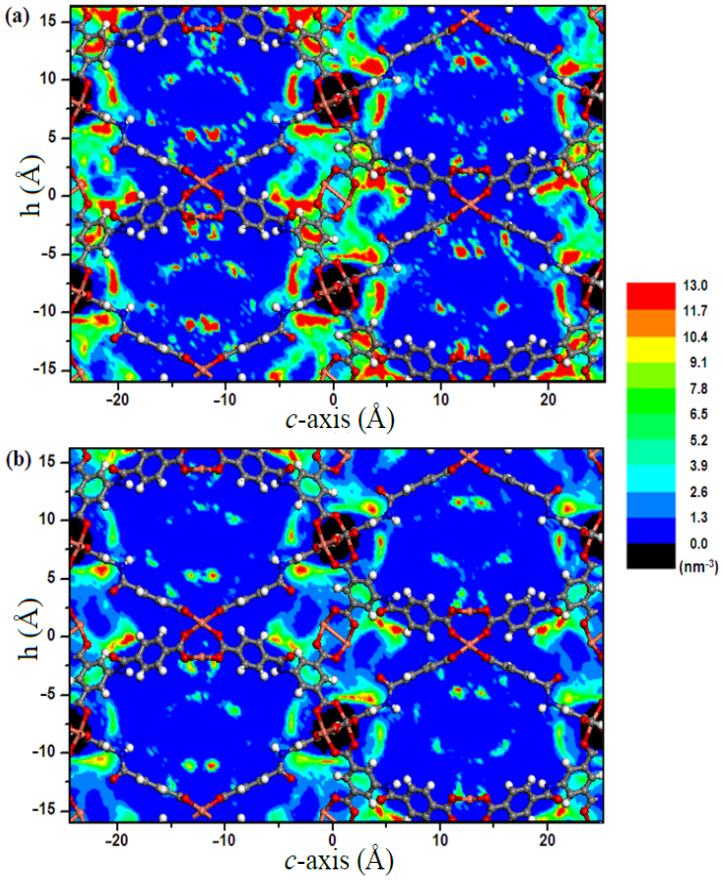

Fig. S1. Density distribution of the center-of-mass of CO_2 molecules perpendicular to *a*-axis of NJU-Bai3: (a) 1.0 atm/273 K and (b) 1.0 atm/298 K.

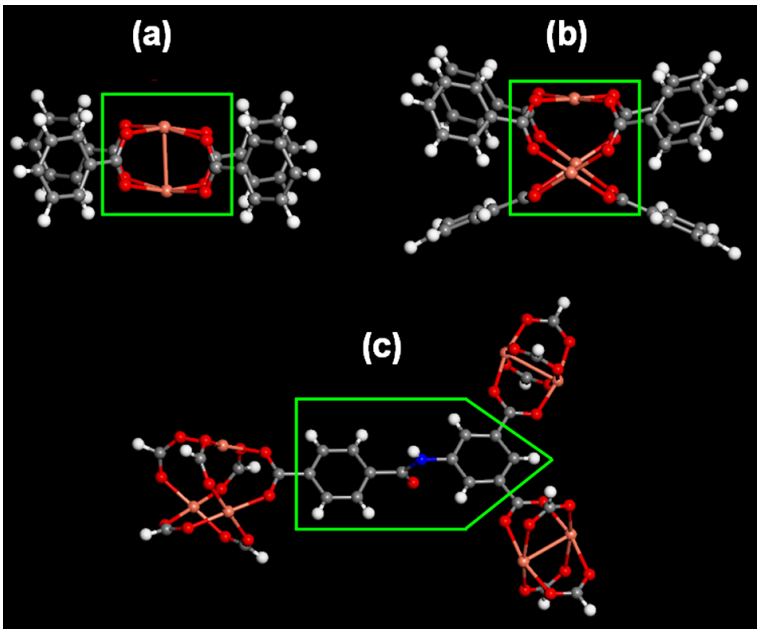

Fig. S2. Structural illustrations of (a) Cluster **A**, (b) Cluster **B**, and (c) Cluster **C**.

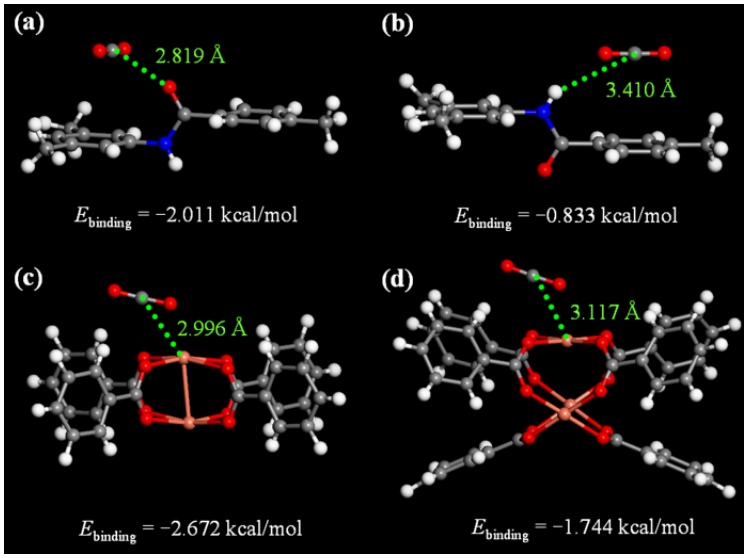

Fig. S3. First-principles calculations for the binding energies of CO_2 molecule at different adsorption sites in NJU-Bai3.

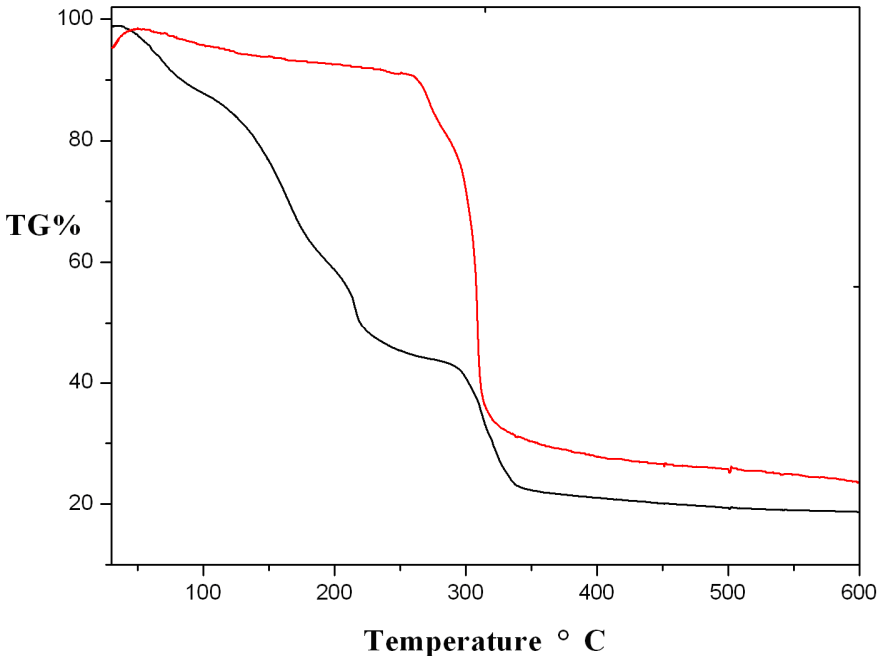

Fig. S4. TG of NJU-Bai3**:** as-synthesized samples (black) and completely activated samples (red).

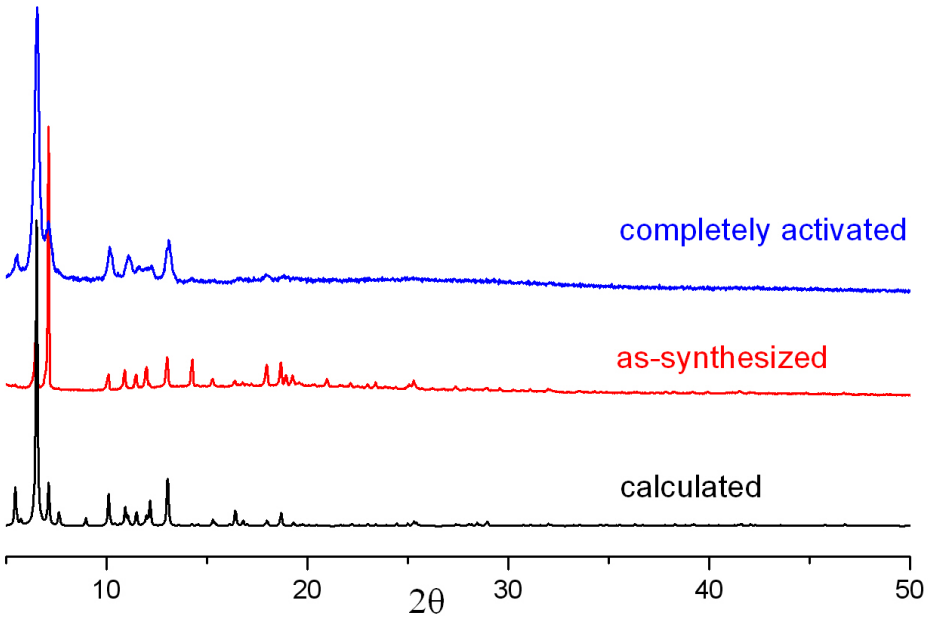

Fig. S5. The PXRD patterns of NJU-Bai3: as-synthesized (red), calculated (black), completely activated samples (blue).

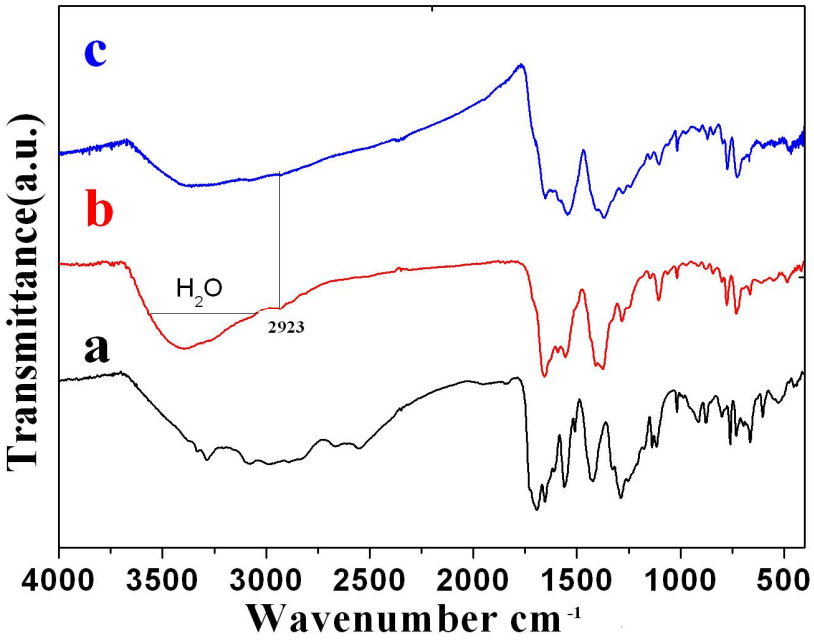

Fig. S6. Infrared spectra. (a) H_3L, (b) as-synthesized NJU-Bai3, (c) activated NJU-Bai3. Note the absence of the vibration frequencies of the solvent DMA, acetone and methanol molecules in the activated samples, and the presence of the peaks around 3400 cm^{-1} in activated samples may result from the rapid re-adsorption of trace moisture during the IR measurements.

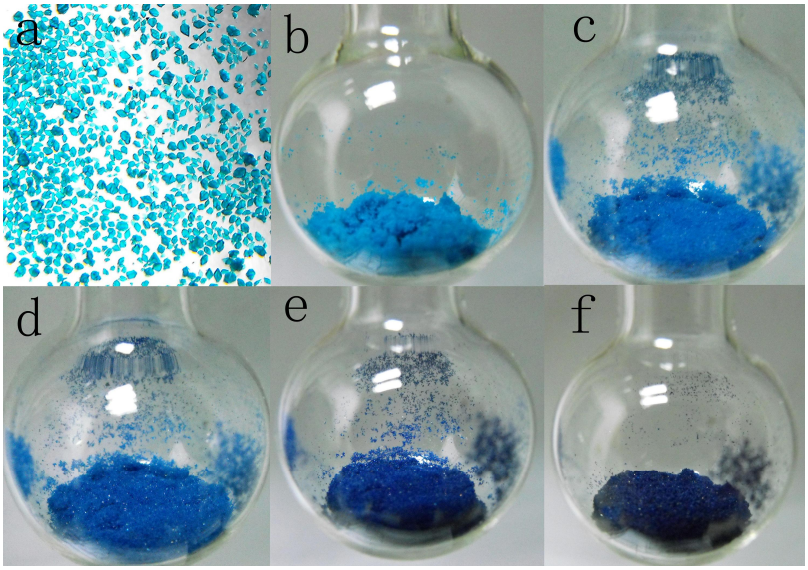

Fig. S7. Photographic images of NJU-Bai3. (a): Crystals of as-synthesized NJU-Bai3. (b-f): Visual observation of colour change in NJU-Bai3 upon activation, and (f) completely activated samples.

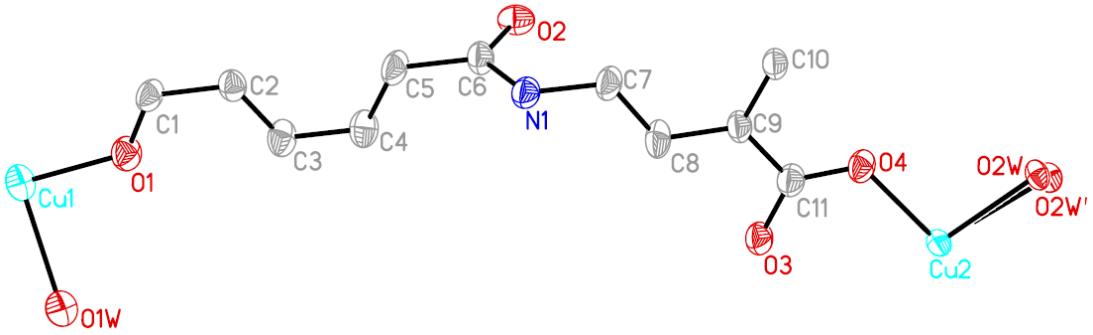

Fig. S8. View of the asymmetric unit for NJU-Bai3**.**

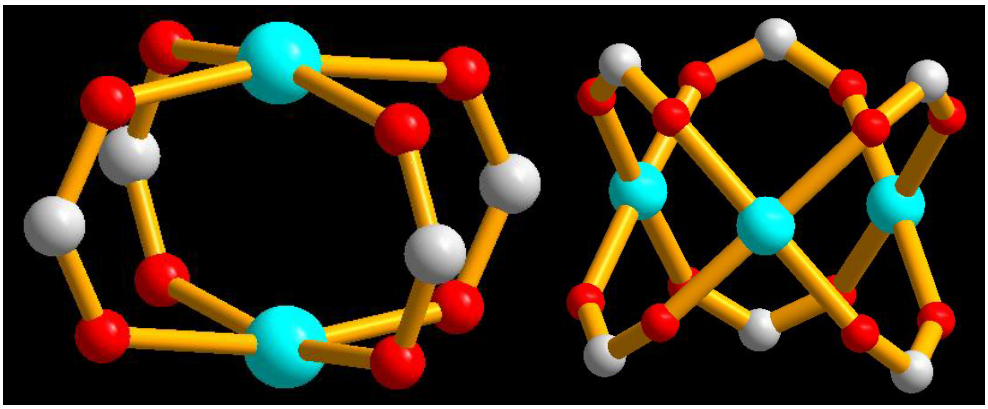

Fig. S9. Two kinds of cluster in NJU-Bai3: $Cu_2(COO)_4$ (left) and $Cu_3(COO)_6$ (right).

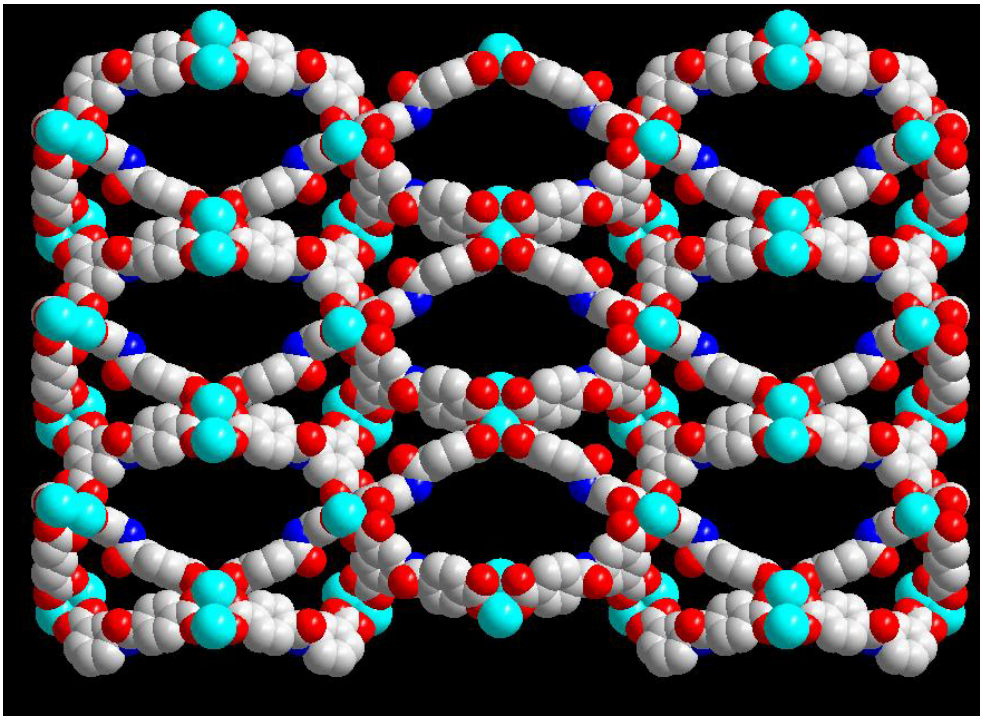

Fig. S10. Large open pore viewed along the *a*-axis of NJU-Bai3**.** Guest molecules and H atoms are omitted for clarity.

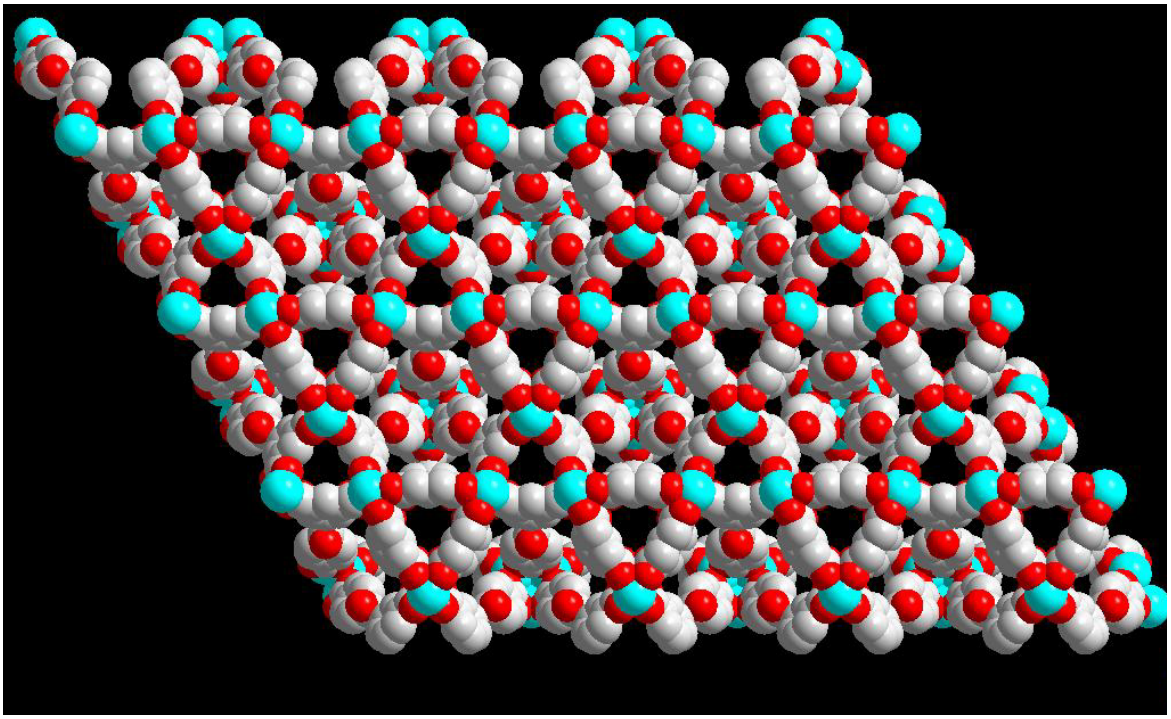

Fig. S11. Large open pore viewed along the *c*-axis of NJU-Bai3**.** Guest molecules and H atoms are omitted for clarity.

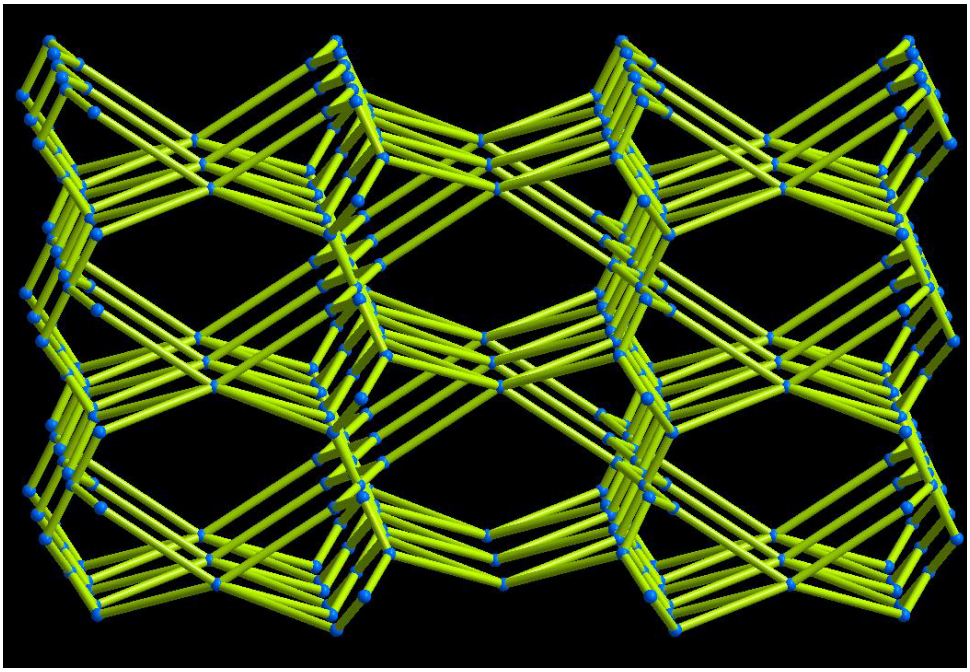

Fig. S12. The *agw*-type network topology of NJU-Bai3

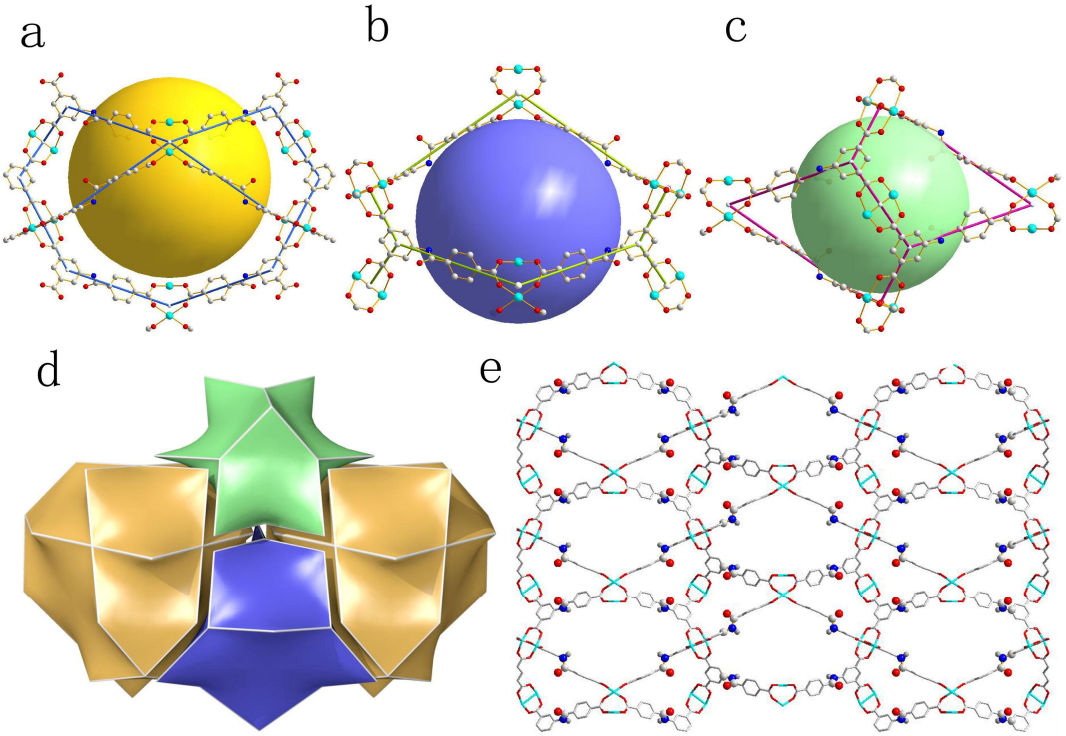

Fig. S13. Three kinds of cage in NJU-Bai3. (a): bowl; (b): hexagonal bipyramidal (c): trigonal bipyramida;); (d): The packed natural tilings of NJU-Bai3; (e): The densely decorated amide groups and exposed open metal sites in the pores from the crystal structure along a-axis

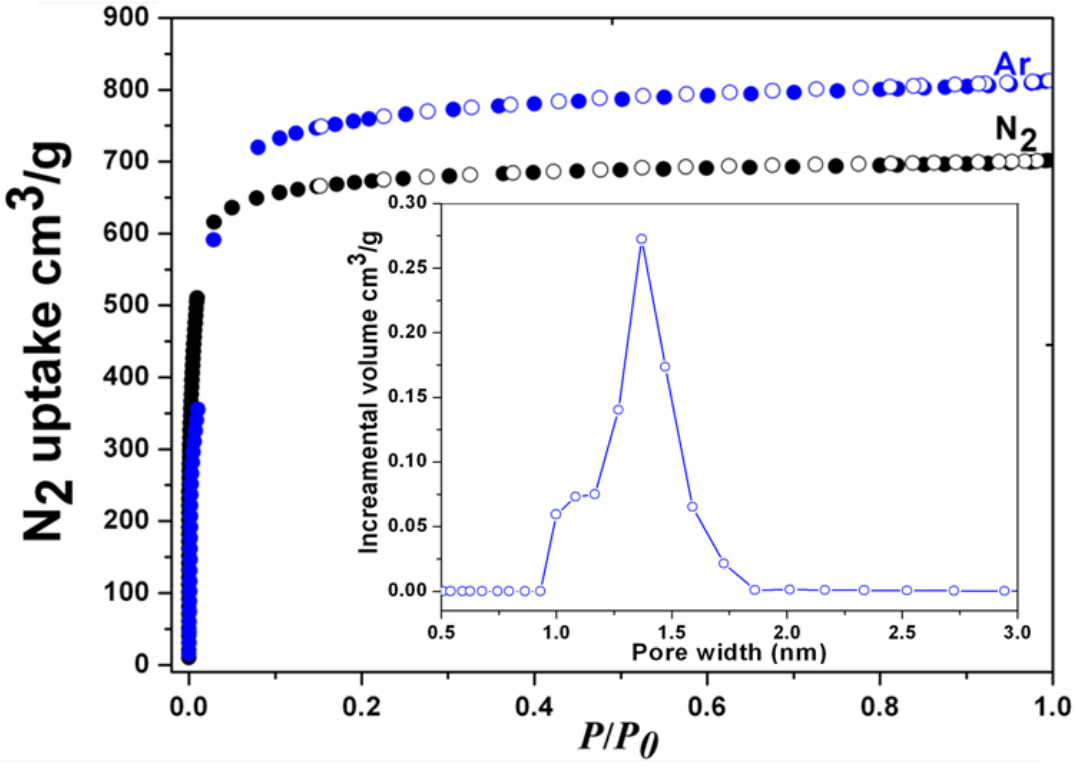

Fig. S14. N_2 and Ar adsorption isotherms of NJU-Bai3 at 77 K and 87K, respectively. Inset: calculated pore size distributions according to Ar isotherm.

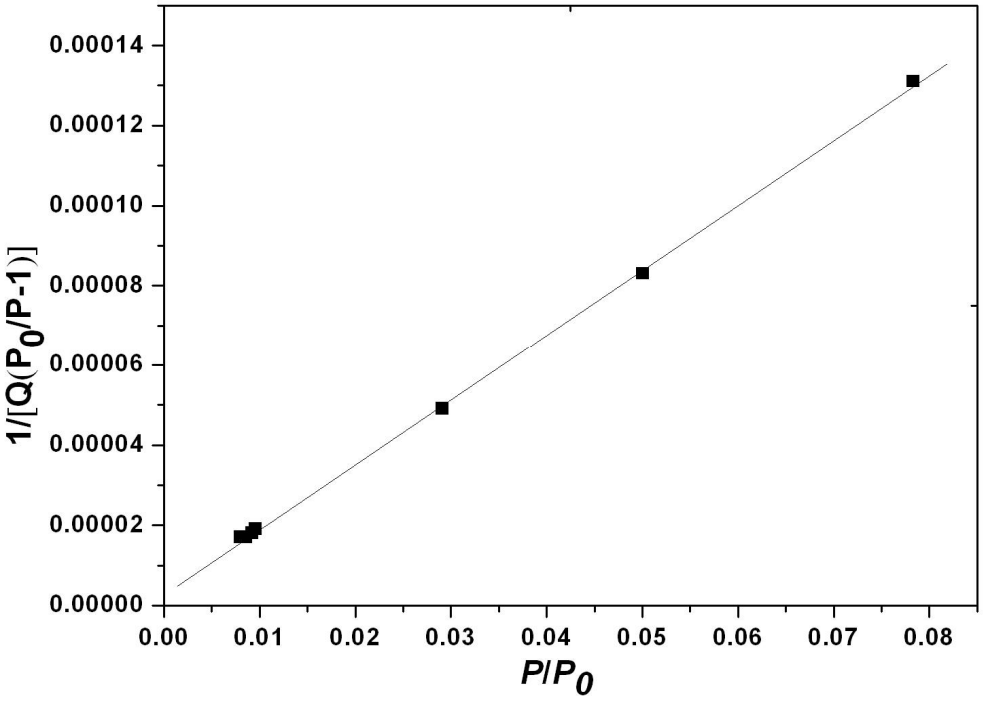

Fig. S15. The BET plot calculated from N_2 isotherm of NJU-Bai3.

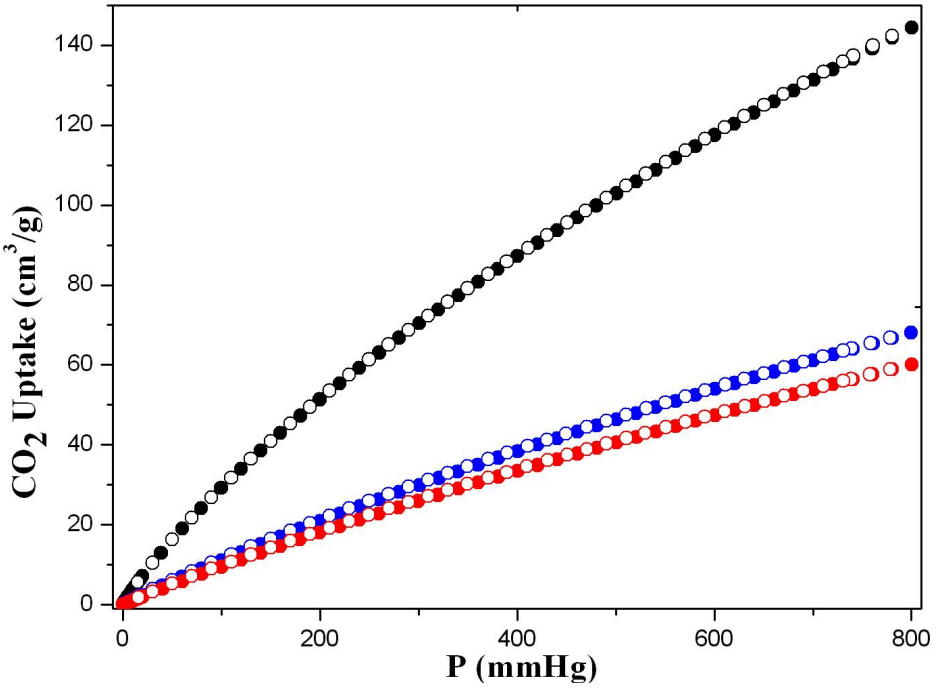

Fig. S16. Low pressure CO_2 adsorption of NJU-Bai3 at 273 (black), 293 (blue) and 298K (red), respectively.

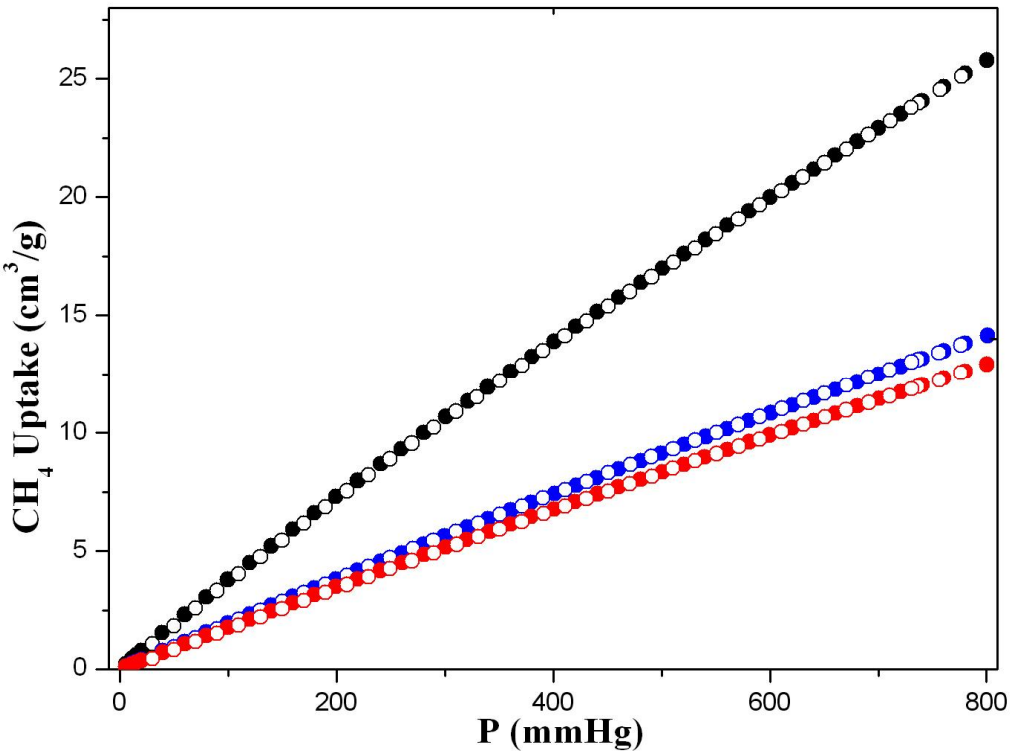

Fig. S17. Low pressure CH_4 adsorption of NJU-Bai3 at 273 (black), 293 (blue) and 298K (red), respectively.

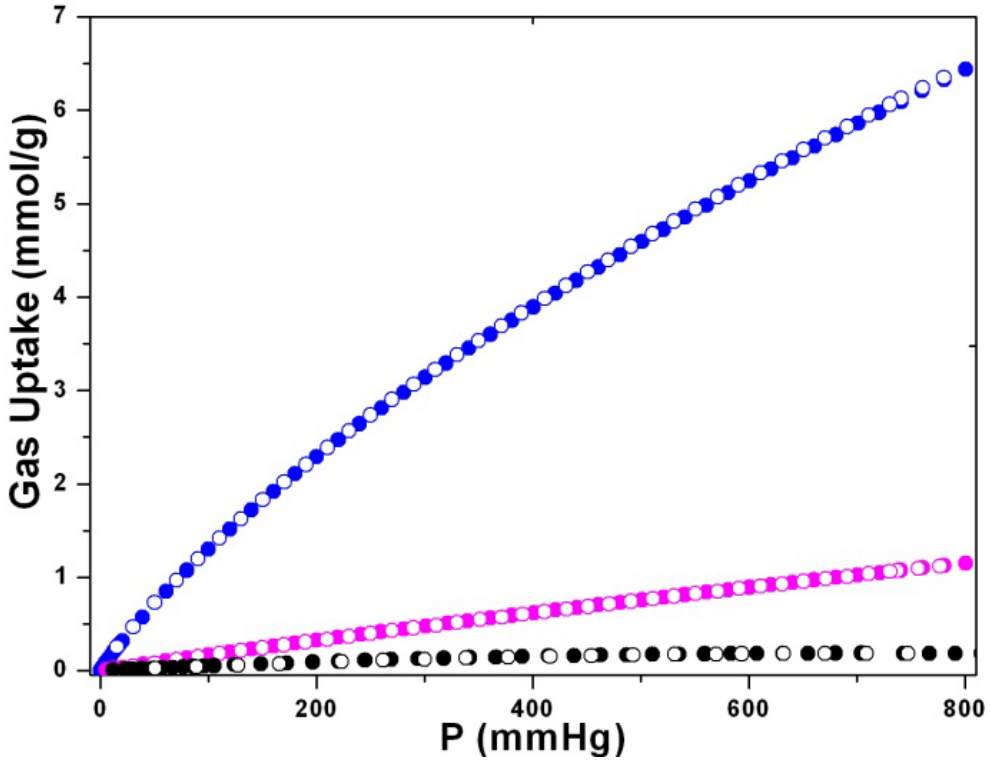

Fig. S18. CO_2 (blue), CH_4 (pink) and N_2 (black) adsorption isotherms of NJU-Bai3 at 273K.

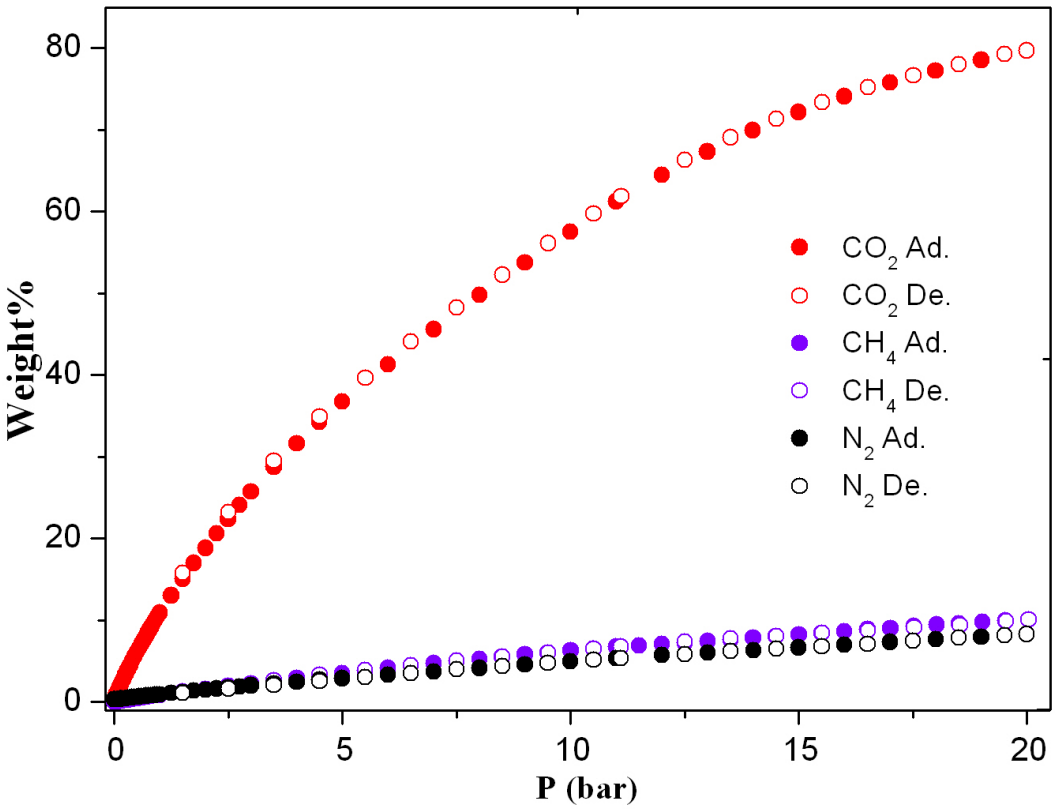

Fig. S19. High pressure gas adsorption isotherms of CO_2, CH_4 and N_2 in NJU-Bai3 at 298 K

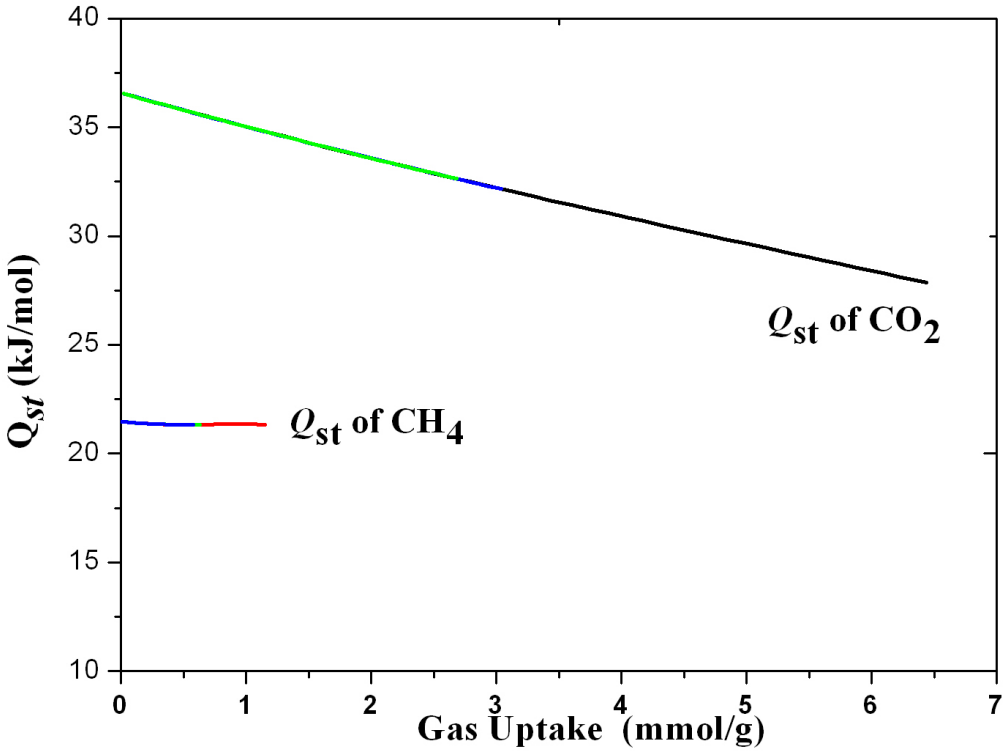

Fig. S20. Isosteric heat of CO_2 and CH_4 adsorption for NJU-Bai3 at low surface coverage.

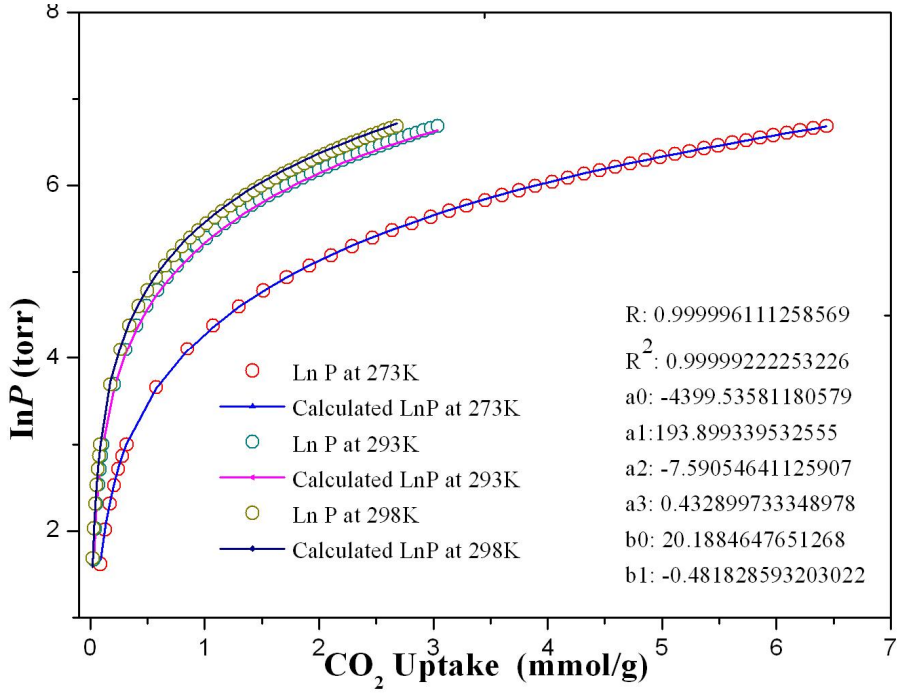

Fig. S21. The calculated virial equation isotherms parameters fit to the experimental CO_2 data of NJU-Bai3.

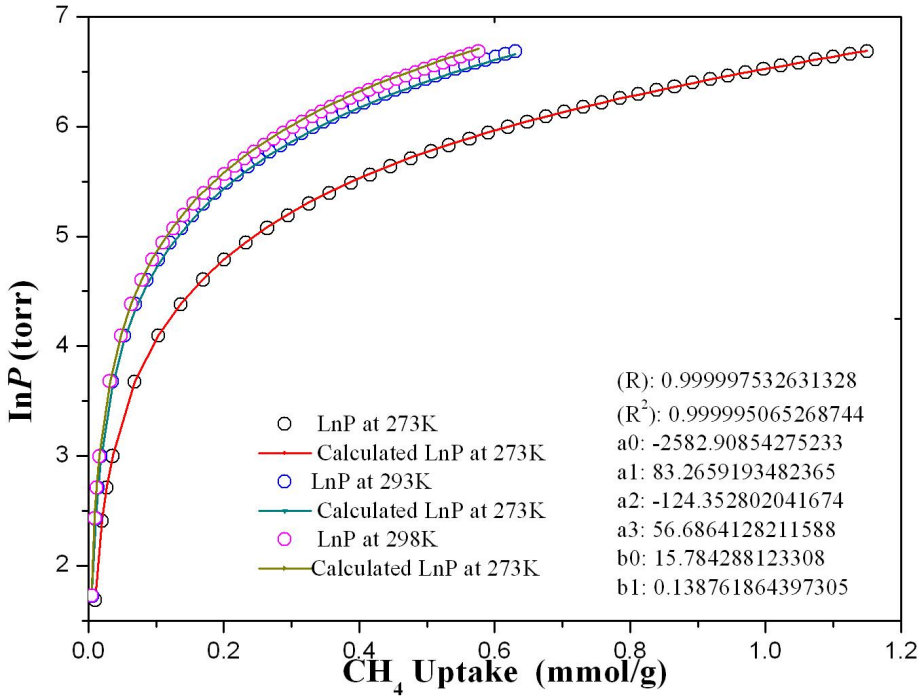

Fig. S22. The calculated virial equation isotherms parameters fit to the experimental CH_4 data of NJU-Bai3.

Table S3. CO_2 uptake and enthalpy of adsorption for MOFs[15] and NJU-Bai3. Asterisks indicate the simulated enthalpy of adsorption due to the lack of experimental data.

Material	CO_2 uptake (mg/g) at 0.1 bar, 298K	$-\triangle H_{ads}$ (kJ/mol)	reference
IRMOF-1	3.5	15.9*	[5]
MOF-177	3.5	15.7*	[5]
UMCM-1	4.1	15.5*	[5]
IRMOF-3	4.9	17.4*	[5]
ZIF-8	5.3	18.7*	[5]
MIL-47	7.8	23.2*	[5]
UMCM-150	11.3	20.3*	[5]
UMCM-150(N)2	12.9	19.7*	[5]
NJU-Bai3	15.1	36.5	This work
Zn-DOBDC	57.4	25.6*	[6]
Mg-DOBDC	261.6	39	[6]

Table S4. N_2 adsorption data of NJU-Bai3 at 77 K.

P/P0	**Ads. cm^3/g**	**P/P0**	**Ads. cm^3/g**	**P/P0**	**Ads. cm^3/g**	**P/P0**	**Des. cm^3/g**
7.60E-07	10.1455	7.38E-04	288.4042	0.12619	661.3495	0.98183	701.1347
1.02E-06	20.2915	8.87E-04	297.4109	0.14863	665.2181	0.96759	700.6234
1.41E-06	30.4369	0.00105	306.2061	0.17122	668.3958	0.95274	700.1907
2.08E-06	40.5816	0.00127	316.2579	0.19182	670.8983	0.9377	699.8173
3.31E-06	50.725	0.0015	326.2953	0.212	673.0544	0.91374	699.3239
6.18E-06	60.8643	0.00176	336.3253	0.24801	676.2434	0.88787	698.8205
1.14E-05	70.9961	0.00202	346.3522	0.30171	679.9783	0.86274	698.3643
1.87E-05	81.1181	0.0023	356.3817	0.36416	683.2946	0.83784	697.9134
2.74E-05	91.2284	0.0026	366.3993	0.39878	684.8049	0.81276	697.4645
3.72E-05	101.326	0.00295	376.3954	0.44936	686.697	0.77513	696.8546
4.82E-05	111.4101	0.00329	386.3901	0.49954	688.2584	0.72536	695.9618
5.98E-05	121.4811	0.00365	396.3883	0.54935	689.6057	0.67531	694.9525
7.19E-05	131.536	0.00402	406.3718	0.59912	690.8067	0.62525	693.8608
8.40E-05	141.5768	0.00442	416.3534	0.6491	691.8418	0.57531	692.6534
9.59E-05	151.6043	0.00485	426.3174	0.69892	692.822	0.52476	691.2747
1.08E-04	161.6177	0.0053	436.2729	0.74903	693.7243	0.47644	688.6623
1.19E-04	171.6157	0.00578	446.215	0.80014	694.5941	0.42221	686.2013
1.32E-04	181.5988	0.00629	456.1445	0.82004	695.0742	0.37533	684.2213
1.45E-04	191.5654	0.00681	466.0233	0.8508	695.6267	0.32567	681.77
1.61E-04	201.5123	0.00738	475.7904	0.87483	696.1252	0.27536	678.6589
1.80E-04	211.4354	0.00799	485.535	0.90034	696.669	0.22542	674.6594
2.04E-04	221.3272	0.00857	495.2809	0.92503	697.2897	0.15193	666.0118
2.36E-04	231.1777	0.00923	504.9868	0.95018	698.0937		
2.78E-04	240.9718	0.00957	510.3128	0.97474	699.368		

3.33E-04	250.694	0.02911	615.6364	0.98043	700.0066		
4.05E-04	260.3221	0.05008	635.943	0.99118	701.0514		
4.95E-04	269.8315	0.07835	649.1638	0.99463	701.6723		
6.07E-04	279.203	0.10502	656.8297				

Table S5. CO_2 adsorption data of NJU-Bai3 at 273, 293 and 298K.

273K CO_2	**Adsorption**		**273-CO_2**	**Desorption**	
P (mmhg)	**Uptake (mmol/g)**	**Uptake (cm3/g)**	**P (mmhg)**	**Uptake (mmol/g)**	**Uptake (cm3/g)**
2.00684	0.03645	0.817	780.32	27.94	142.3294
2.45631	0.04439	0.9949	760.8844	27.459	139.8791
5.03575	0.08759	1.9633	741.1193	26.955	137.3114
7.5118	0.12887	2.8885	730.2487	26.67	135.8618
10.11864	0.16982	3.8064	710.8131	26.163	133.2798
12.49	0.20688	4.6371	690.6654	25.63	130.5618
15.09793	0.24597	5.5131	670.3378	25.085	127.7846
17.52786	0.28166	6.3131	650.6856	24.551	125.0675
20.06627	0.3178	7.1231	630.5295	23.998	122.2486
38.80936	0.57421	12.8703	610.7896	23.449	119.4529
60.53405	0.8472	18.9891	590.4268	22.878	116.5437
79.70918	1.07402	24.0733	570.8397	22.323	113.7149
99.86053	1.30045	29.1484	550.6668	21.749	110.7918
119.8963	1.5146	33.9484	530.7902	21.169	107.8365
139.6895	1.71791	38.5053	510.5566	20.575	104.8106
159.9404	1.91764	42.9822	490.9078	19.987	101.8161
180.0859	2.10892	47.2696	469.6583	19.347	98.5581
199.7501	2.28968	51.3212	450.8164	18.771	95.6241
219.9112	2.46923	55.3455	430.3622	18.142	92.4159
239.7803	2.64108	59.1975	411.0331	17.529	89.2927
260.1552	2.81239	63.0373	389.5691	16.847	85.8229
280.4937	2.97949	66.7827	370.8566	16.238	82.7188
300.6625	3.14108	70.4045	349.8414	15.543	79.1763
319.806	3.29071	73.7583	329.8571	14.869	75.7463
340.7783	3.45201	77.3738	309.7047	14.182	72.2431
360.535	3.60067	80.7057	289.8263	13.487	68.703
380.5902	3.74924	84.0358	269.8123	12.771	65.0558
400.3796	3.89367	87.273	249.8797	12.038	61.3224
420.7245	4.03902	90.5311	229.8077	11.281	57.4657
440.3766	4.17813	93.6489	209.9019	10.509	53.5348
460.8942	4.3208	96.8468	189.9414	9.712	49.4743
480.3776	4.45408	99.8342	169.9583	8.891	45.2937
500.8195	4.592	102.9255	150.0711	8.045	40.9805
520.7337	4.724	105.8842	130.0386	7.157	36.4588
540.5375	4.85475	108.8149	110.0365	6.237	31.7698
560.3588	4.9839	111.7097	90.12212	5.277	26.8797
580.7019	5.11586	114.6674	70.08082	4.264	21.7232

600.3199	5.24188	117.4921	50.14553	3.2	16.3012
620.3067	5.36766	120.3112	30.19709	2.057	10.4789
640.2314	5.49075	123.0701	15.06825	1.111	5.66
660.6021	5.61628	125.8839	--	--	--
680.5374	5.73719	128.5939	--	--	--
700.7275	5.85897	131.3235	--	--	--
720.1584	5.9748	133.9198	--	--	--
740.5631	6.09387	136.5886	--	--	--
760.1792	6.20835	139.1546	--	--	--
780.5707	6.3256	141.7826	--	--	--
293K CO2	**Adsorption**		**293-CO2**	**Desorption**	
P (mmhg)	**Uptake (mmol/g)**	**Uptake (cm3/g)**	**P (mmhg)**	**Uptake (mmol/g)**	**Uptake (cm3/g)**
2.01213	0.01049	0.235	778.6569	2.97857	66.762
2.4858	0.0131	0.2936	758.6196	2.91916	65.4304
5.30711	0.0288	0.6456	739.0903	2.86057	64.117
7.58413	0.0416	0.9323	730.7175	2.8342	63.526
10.08289	0.05557	1.2455	710.1975	2.77152	62.121
12.60247	0.06896	1.5457	690.898	2.71124	60.77
15.04146	0.08232	1.8452	670.7389	2.64762	59.344
17.60926	0.09577	2.1465	650.5433	2.58374	57.9123
20.04107	0.10861	2.4344	630.6805	2.52017	56.4872
40.17251	0.2105	4.7181	611.1762	2.4572	55.0759
60.10194	0.30781	6.8993	590.5922	2.39027	53.5758
79.98482	0.40212	9.0132	570.545	2.32432	52.0976
100.1904	0.49535	11.1028	550.6433	2.25875	50.6279
119.9562	0.58461	13.1035	530.9647	2.19254	49.1438
139.8903	0.67318	15.0887	510.3682	2.12219	47.5671
159.8025	0.75985	17.0314	490.8149	2.05491	46.0589
179.8287	0.84539	18.9488	470.6145	1.98509	44.4939
200.2449	0.93116	20.871	449.707	1.91145	42.8435
219.8034	1.01242	22.6926	430.5168	1.84284	41.3057
240.3597	1.09622	24.5708	410.7359	1.77228	39.724
259.6881	1.17402	26.3147	389.7281	1.69566	38.0067
280.2124	1.2557	28.1453	370.5724	1.62498	36.4225
300.6563	1.33594	29.9438	349.7228	1.54691	34.6727
320.7473	1.41332	31.6782	329.7513	1.47092	32.9693
339.6573	1.48548	33.2958	309.6822	1.39371	31.2387
360.1655	1.56278	35.0283	289.7719	1.31627	29.5031
380.7946	1.6397	36.7523	269.659	1.23664	27.7181
400.6	1.71319	38.3996	249.8778	1.15776	25.9501
420.8905	1.78668	40.0469	229.8401	1.07613	24.1204
440.4691	1.85737	41.6313	209.8805	0.99348	22.2679
461.0277	1.92991	43.2572	189.8621	0.90925	20.38
480.7477	1.99939	44.8146	169.9477	0.82442	18.4787
500.8619	2.06953	46.3867	150.0127	0.73778	16.5367
520.8849	2.13866	47.9362	130.0031	0.64944	14.5567
540.3212	2.20493	49.4216	110.0463	0.5594	12.5384

560.7645	2.27383	50.9659	90.06015	0.4669	10.4651
580.7434	2.34014	52.4522	70.05254	0.37222	8.3429
600.5568	2.40612	53.9309	50.08697	0.27533	6.1712
620.4787	2.47141	55.3944	30.1451	0.17461	3.9138
640.4161	2.5362	56.8467	15.09575	0.0947	2.1226
660.5651	2.6012	58.3036			
680.6805	2.66562	59.7475			
700.4125	2.72812	61.1484			
720.5997	2.79184	62.5765			
740.707	2.85491	63.9901			
760.9122	2.917	65.3819			
780.1821	2.97686	66.7236			
799.9016	3.03697	68.0709			
298K CO2	**Adsorption**		**298-CO2**	**Desorption**	
P (mmhg)	**Uptake (mmol/g)**	**Uptake (cm3/g)**	**P (mmhg)**	**Uptake (mmol/g)**	**Uptake (cm3/g)**
2.01223	0.0057	0.1278	778.1694	2.62431	58.8215
2.48343	0.00772	0.173	758.0507	2.57026	57.61
5.38426	0.02124	0.4762	738.7382	2.51757	56.4291
7.63458	0.03193	0.7158	730.8562	2.49594	55.9442
10.13114	0.04295	0.9627	710.5634	2.44061	54.7042
12.54384	0.05402	1.2108	690.3767	2.38463	53.4494
15.10496	0.06582	1.4754	670.8032	2.32991	52.2229
17.60213	0.07682	1.7219	651.016	2.27354	50.9594
20.06861	0.08766	1.9649	630.8596	2.21615	49.673
40.08938	0.17503	3.9232	610.5112	2.15745	48.3572
60.25737	0.2602	5.8321	590.4039	2.09844	47.0346
80.0006	0.34123	7.6483	570.8181	2.04051	45.7361
99.95513	0.42138	9.4448	550.7131	1.98067	44.395
119.9107	0.49998	11.2065	529.6347	1.9176	42.9813
139.9233	0.57766	12.9477	510.8113	1.86029	41.6967
159.9306	0.65357	14.6491	490.674	1.79893	40.3213
179.8034	0.72789	16.3149	470.7074	1.73696	38.9325
199.7031	0.80125	17.9592	450.7332	1.67472	37.5374
219.836	0.87464	19.6043	430.8049	1.61149	36.1201
239.6803	0.94571	21.1971	409.7183	1.54355	34.5972
259.6743	1.01636	22.7809	389.5943	1.47839	33.1369
279.7443	1.08654	24.3538	370.6719	1.41635	31.7462
299.6616	1.15556	25.9008	349.6878	1.34665	30.184
319.6476	1.22402	27.4354	329.6782	1.2796	28.6811
340.6011	1.29442	29.0133	309.6395	1.2116	27.1569
360.5693	1.36144	30.5155	289.6603	1.14281	25.6151
381.0536	1.42857	32.02	269.8677	1.07408	24.0746
400.5938	1.4926	33.4553	249.7779	1.00332	22.4884
420.6335	1.55722	34.9036	229.8394	0.93198	20.8896
440.4516	1.62075	36.3277	209.7919	0.8594	19.2627
460.9305	1.68543	37.7774	189.9472	0.78659	17.6307
480.8932	1.74798	39.1795	169.9479	0.71178	15.9539

500.8057	1.81022	40.5744	149.9629	0.63559	14.2461
521.0863	1.87238	41.9678	129.9736	0.55852	12.5188
541.0247	1.93345	43.3365	110.0577	0.48029	10.7652
560.8192	1.99333	44.6788	90.06458	0.39974	8.9598
580.7282	2.0533	46.0228	70.04671	0.31752	7.117
600.7404	2.1129	47.3588	50.09976	0.23362	5.2365
620.7892	2.17122	48.666	30.13796	0.14648	3.2831
640.4729	2.22918	49.9651	15.65205	0.08004	1.794
661.2153	2.28921	51.3106			
680.6199	2.3456	52.5745			
700.9012	2.40319	53.8653			
720.3199	2.45833	55.1012			
740.3995	2.51434	56.3567			
760.3136	2.57024	57.6097			
780.4308	2.62578	58.8545			
800.3549	2.6808	60.0878			

Table S6. CH_4 adsorption data of NJU-Bai3 at 273, 293 and 298K.

273K CH4	**Adsorption**		**273-CH4**	**Desorption**	
P (mmhg)	**Uptake (mmol/g)**	**Uptake (cm3/g)**	**P (mmhg)**	**Uptake (mmol/g)**	**Uptake (cm3/g)**
5.41152	0.00972	0.2178	776.8099	1.12004	25.1047
11.10476	0.01988	0.4457	756.921	1.09474	24.5376
15.07883	0.02689	0.6028	737.0944	1.06909	23.9626
20.06131	0.03561	0.7982	730.3287	1.06043	23.7686
39.35777	0.06852	1.5359	710.9971	1.0356	23.2121
59.98529	0.1034	2.3176	691.0363	1.00951	22.6272
79.92257	0.13633	3.0558	670.8839	0.98292	22.0312
99.88527	0.16911	3.7904	650.7037	0.95632	21.435
119.7881	0.20091	4.5032	630.3944	0.92965	20.8372
139.8097	0.23253	5.2119	610.8375	0.9037	20.2556
159.8346	0.26414	5.9205	590.8723	0.87751	19.6685
179.6267	0.29473	6.6061	571.121	0.85075	19.0687
199.7245	0.32561	7.2983	550.4278	0.82276	18.4414
219.6717	0.35588	7.9766	530.8541	0.79624	17.8471
240.8758	0.3878	8.6923	511.0674	0.76945	17.2465
259.6394	0.41594	9.3229	490.9668	0.74173	16.6253
280.5796	0.44644	10.0065	470.6523	0.71366	15.9959
300.9665	0.47648	10.6798	451.1151	0.68597	15.3755
321.2338	0.50601	11.3417	431.0402	0.65818	14.7525
339.6082	0.53253	11.9362	410.8032	0.62989	14.1184
360.8718	0.56292	12.6174	390.6442	0.60155	13.4832
380.6216	0.59083	13.2428	371.3974	0.57406	12.8669
400.9493	0.61969	13.8899	350.979	0.54472	12.2094

421.0997	0.64807	14.526	329.6779	0.51387	11.5179
440.8511	0.67564	15.144	310.6949	0.48641	10.9025
460.6182	0.70311	15.7595	289.6404	0.4557	10.2141
480.8986	0.73093	16.3832	269.7105	0.42621	9.5531
500.9869	0.7583	16.9967	249.6216	0.39647	8.8865
520.8765	0.7854	17.604	229.7281	0.3664	8.2126
540.5108	0.81196	18.1994	209.7543	0.33624	7.5365
560.7086	0.83903	18.8061	189.6713	0.30575	6.8531
580.7636	0.86575	19.4049	169.8499	0.27485	6.1605
600.4707	0.89195	19.9921	149.8118	0.24336	5.4547
620.5956	0.9185	20.5874	129.9103	0.21209	4.7537
640.4712	0.94467	21.1738	109.9997	0.1802	4.0391
660.2982	0.97071	21.7577	89.97888	0.14801	3.3174
680.7428	0.99718	22.3508	70.07845	0.11523	2.5829
700.3193	1.02239	22.9159	50.0554	0.08177	1.8327
720.8412	1.04893	23.5108	30.10785	0.04746	1.0638
740.3714	1.07389	24.0702	--	--	--
760.5114	1.09984	24.652	--	--	--
780.5599	1.12505	25.217	--	--	--
800.4023	1.1499	25.774	--	--	--
293K CH4	**Adsorption**		**293-CH4**	**Desorption**	
P (mmhg)	**Uptake (mmol/g)**	**Uptake (cm3/g)**	**P (mmhg)**	**Uptake (mmol/g)**	**Uptake (cm3/g)**
5.61773	0.00553	0.124	776.3238	0.61274	13.734
11.35579	0.01062	0.2381	756.0653	0.59806	13.405
15.07296	0.01363	0.3056	736.7664	0.58456	13.1023
20.06539	0.01775	0.3978	730.7924	0.58029	13.0067
39.52572	0.03474	0.7786	710.5426	0.56539	12.6728
60.06329	0.05254	1.1776	690.781	0.55131	12.3572
79.96213	0.06945	1.5567	670.9234	0.53651	12.0254
99.82451	0.08642	1.9371	650.4037	0.52114	11.6809
119.9134	0.10349	2.3196	631.0676	0.50691	11.362
139.8031	0.12045	2.6997	611.1581	0.49201	11.028
159.7943	0.1369	3.0685	590.77	0.47651	10.6806
179.6151	0.15307	3.4309	570.6129	0.46113	10.3358
199.6752	0.16967	3.8031	550.8729	0.44655	10.009
219.615	0.18593	4.1675	531.0907	0.4315	9.6716
240.9318	0.20307	4.5516	510.8358	0.416	9.3244
260.25	0.21912	4.9114	490.6735	0.40089	8.9856
280.6834	0.23562	5.2812	471.3925	0.38626	8.6576
299.7397	0.25102	5.6264	451.0352	0.37021	8.298
320.879	0.26798	6.0066	430.7909	0.35424	7.94
340.0557	0.28341	6.3525	411.2017	0.33879	7.5937

360.7814	0.2997	6.7176	390.905	0.32282	7.2357
379.751	0.31461	7.0517	371.4124	0.30748	6.8918
401.3746	0.33138	7.4276	351.1006	0.29161	6.5363
421.1754	0.34669	7.7709	330.8209	0.27544	6.1739
439.7983	0.361	8.0915	310.6651	0.25953	5.8172
460.7137	0.37727	8.4561	289.5928	0.24272	5.4402
480.9755	0.39277	8.8037	270.8441	0.22753	5.0999
499.5895	0.4072	9.127	249.6362	0.20997	4.7063
521.2062	0.42364	9.4955	229.5913	0.19343	4.3356
540.97	0.43856	9.83	209.7065	0.17708	3.9691
560.7459	0.45337	10.1619	189.7583	0.16037	3.5945
580.6202	0.46832	10.497	169.8421	0.14399	3.2275
600.8677	0.48348	10.8368	149.8926	0.12732	2.8538
620.8998	0.49842	11.1715	129.9588	0.11048	2.4762
640.8734	0.51288	11.4958	110.0302	0.09331	2.0915
660.731	0.52765	11.8268	89.97371	0.07611	1.706
680.445	0.54231	12.1555	70.0932	0.05878	1.3176
700.4141	0.55694	12.4834	50.03618	0.04166	0.9339
720.891	0.57177	12.8158	--	--	--
740.3233	0.58643	13.1444			
760.8427	0.60149	13.4819			
780.7131	0.61616	13.8106			
800.799	0.63071	14.1368			
298K CH4	**Adsorption**		**298-CH4**	**Desorption**	
P (mmhg)	**Uptake (mmol/g)**	**Uptake (cm3/g)**	**P (mmhg)**	**Uptake (mmol/g)**	**Uptake (cm3/g)**
5.63506	0.0049	0.1099	776.1843	0.55978	12.547
11.37512	0.00957	0.2145	756.4498	0.54643	12.2477
15.07534	0.01226	0.2748	736.7289	0.53363	11.9607
20.03521	0.01621	0.3634	730.8132	0.52939	11.8658
39.57932	0.03173	0.7111	710.4562	0.51573	11.5597
59.98021	0.04787	1.0729	691.1962	0.50296	11.2733
79.97069	0.06345	1.4221	670.4287	0.48893	10.959
99.82003	0.07881	1.7664	650.9032	0.47554	10.6588
119.8454	0.09457	2.1197	630.9169	0.46162	10.3469
139.7539	0.10989	2.463	610.8525	0.4474	10.028
159.6665	0.12511	2.8043	590.8864	0.43409	9.7298
179.652	0.1405	3.1491	571.2626	0.42054	9.4259
199.694	0.15555	3.4865	550.937	0.4066	9.1135
219.5602	0.17028	3.8166	531.0745	0.393	8.8088
240.7407	0.18618	4.1731	510.7088	0.37862	8.4865
260.8462	0.20102	4.5058	491.1094	0.36391	8.1567
281.1693	0.21598	4.8411	470.7401	0.34979	7.8401

301.0221	0.2305	5.1665	451.0248	0.33596	7.5303
320.2077	0.24469	5.4845	430.7198	0.32136	7.2029
341.6213	0.25966	5.82	410.9938	0.30746	6.8914
360.9196	0.27366	6.1339	391.3581	0.29308	6.5692
379.7809	0.28737	6.4412	371.0961	0.2785	6.2423
400.9866	0.30229	6.7757	350.6005	0.2638	5.9128
420.0763	0.3159	7.0807	331.2519	0.24988	5.6009
440.9968	0.33064	7.4109	311.3832	0.23533	5.2747
460.0851	0.34392	7.7087	289.6288	0.21934	4.9162
480.6946	0.35821	8.029	269.7038	0.20447	4.5829
500.946	0.37246	8.3484	249.6362	0.18955	4.2487
521.0396	0.38648	8.6627	229.6162	0.17447	3.9106
539.6552	0.39994	8.9643	209.6243	0.15925	3.5695
560.8353	0.41454	9.2915	189.7404	0.14442	3.2371
581.1422	0.42856	9.6058	169.9026	0.12907	2.8931
599.5715	0.44135	9.8925	149.8336	0.11363	2.5469
620.5236	0.4554	10.2073	129.9676	0.09858	2.2097
640.5872	0.46918	10.5162	109.9918	0.08281	1.8562
660.8387	0.48305	10.8272	89.95737	0.06732	1.5089
680.8165	0.49652	11.1291	70.07288	0.05192	1.1636
701.0582	0.51082	11.4496	50.08558	0.03615	0.8102
720.6846	0.52382	11.741	30.08056	0.02022	0.4532
740.4088	0.53683	12.0326			
760.4249	0.55003	12.3284			
780.5271	0.56308	12.6209			
800.5009	0.57606	12.9119			

Table S7. High pressure adsorption data of NJU-Bai3 at 273K

High pressure CO2 adsorption at 273K		**High pressure N2 adsorption at 273K**		**High pressure CH4 adsorption at 273K**	
P(KPa)Ad	**wt%**	**P(KPa)Ad**	**wt%**	**P(KPa)Ad**	**wt%**
10.313	0.51705	10.713	0.00269	10.447	2.10E-04
18.17	0.81699	19.102	0.01101	18.303	0.01803
29.223	1.19432	39.876	0.02826	30.022	0.0399
38.278	1.51272	59.451	0.04504	39.743	0.05813
59.718	2.20638	79.426	0.062	60.117	0.09715
79.426	2.79412	99.268	0.07882	80.492	0.13363
99.667	3.40562	149.604	0.12097	100.866	0.16729
125.102	4.1183	199.009	0.16556	126.301	0.20678
150.137	4.81725	297.684	0.24819	151.336	0.25919
174.906	5.45006	397.425	0.33338	175.439	0.29474
200.207	6.10671	498.764	0.41822	200.341	0.33196
250.278	7.3244	598.638	0.50118	248.813	0.40693
299.282	8.46881	698.513	0.58269	298.617	0.47896

349.752	9.58554	798.253	0.66376	348.82	0.54962
398.624	10.63048	898.128	0.7443	399.157	0.62052
449.227	11.66657	998.135	0.8247	449.493	0.68982
499.696	12.67534	1497.505	1.21718	499.563	0.75842
548.968	13.6301	1998.074	1.59733	548.701	0.82458
599.97	14.57158	2497.178	1.96692	599.837	0.89254
648.575	15.46129	2997.747	2.32577	648.176	0.95679
699.045	16.36621	3497.118	2.6748	698.513	1.0232
748.849	17.23583	3997.953	3.01677	748.583	1.08742
799.052	18.10288	4497.058	3.34927	798.653	1.15149
848.723	18.95053	4997.094	3.6745	847.658	1.21461
899.06	19.77591	5496.864	3.99322	898.793	1.27886
948.065	20.57304	5997.699	4.30472	948.331	1.33991
998.934	21.38713	6496.803	4.60885	998.268	1.40266
1247.82	25.13469	6997.772	4.90565	1248.752	1.7107
1497.106	28.61033	7496.343	5.19618	1497.638	2.00979
1747.324	31.82618	7997.312	5.48178	1748.123	2.29945
1997.542	34.76964	8496.416	5.76306	1998.474	2.58216
2247.893	37.48545	8996.984	6.03371	2248.958	2.85649
2496.779	39.99665	9496.089	6.2997	2498.111	3.12324
2747.13	42.3736	9996.658	6.56054	2748.462	3.3843
2996.949	44.675	10495.9	6.8171	2998.679	3.64063
3495.387	49.10679	10995.13	7.06917	3498.05	4.1341
3996.222	53.53074	11495.97	7.31743	3998.752	4.60989
4494.793	58.05957	11994.67	7.55821	4498.389	5.06686
4995.762	62.65408	12494.71	7.79726	4998.958	5.50811
5995.036	71.00792	12993.68	8.02928	5998.897	6.34062
6994.975	77.21576	13494.92	8.26097	6998.704	7.1113
7994.382	81.49244	13993.89	8.48464	7998.51	7.83045
8993.789	84.56487	14494.45	8.70831	8999.516	8.49702
9991.997	86.90173	14992.49	8.92065	9998.123	9.13219
10991.67	88.77686	15494.53	9.1338	10997.4	9.72226
11991.34	90.30298	15991.77	9.34327	12000.67	10.28453
12989.02	91.62669	16493.67	9.5493	13009.13	10.81462
13986.69	92.75535	16993.04	9.75339	14019.32	11.31776
14984.37	93.78682	17493.21	9.94897	15039.77	11.7886
15984.98	94.63189	17993.51	10.14478	16069.67	12.24579
16983.72	95.44734	18493.95	10.33751	17106.49	12.70009
17981.26	96.14774	18993.85	10.52486	17999.37	13.05619
18983.2	96.77126	19497.88	10.71222	19022.61	13.41362
19983.67	97.34232	19997.39	10.8916	20023.75	13.7845

References:

[1] P. Cavalleri, N. N. Chavan, A. Ciferri, C. DellErba, A. E. Lozano, M. Novi, J. Preston, *Macromolecules* 1997, **30,** 3112.

[2] G. M. Sheldrick, *Acta Crystallogr., Sect. A:* 2008, **64**, 112.

[3] a)P. Vandersluis, A. L. Spek, *Acta Crystallogr A* 1990, **46**, 194; b)A. L. Spek, *J Appl Crystallogr* 2003, **36**, 7.

[4] Y. Yan, X. Lin, S. H. Yang, A. J. Blake, A. Dailly, N. R. Champness, P. Hubberstey, M. Schroder, *Chem. Commun.* **2**009, 1025.

[5] J. L. C. Rowsell, O. M. Yaghi, *J. Am. Chem. Soc.* 2006, **128**, 1304.

[6] a)R. Babarao, Z. Q. Hu, J. W. Jiang, S. Chempath, S. I. Sandler, *Langmuir* 2007, **23**, 6596; b)V. Goetz, O. Pupier, A. Guillot, *Adsorption* 2006, **12**, 55.

[7] J. G. Harris, K. H. Yung, *J. Phys. Chem.* **1995**, **99**, 12021.

[8] A. K. Rappe, C. J. Casewit, K. S. Colwell, W. A. Goddard, W. M. Skiff, *J. Am. Chem.Soc.*1992, **114**, 10024.

[9] M. S. Santosh, A. P. Lyubartsev, A. A. Mirzoev, D. K. Bhat, *J.Phy.Chem. B* 2010, **114,** 16632.

[10] a)R. Babarao, J. W. Jiang, *J. Am. Chem. Soc.* 2009, **131**, 11417; b)O. K. Farha, A. O. Yazaydin, I. Eryazici, C. D. Malliakas, B. G. Hauser, M. G. Kanatzidis, S. T. Nguyen, R. Q. Snurr, J. T. Hupp, *Nat. Chem.* 2010, **2**, 944; c)R. Vaidhyanathan, S. S. Iremonger, G. K. H. Shimizu, P. G. Boyd, S. Alavi, T. K. Woo, *Science* 2010, **330**, 650.

[11] a)U. C. Singh, P. A. Kollman, *J. Comput. Chem.* 1984, *5*, 129-145; b)B. H. Besler, K. M. Merz, P. A. Kollman, *J. Comput. Chem.* 1990, **11**, 431.

[12] B. Widom, *J. Chem. Phy.* 1963, **39,** 2808.

[13] J. I. Siepmann, D. Frenkel, *Mol. Phy.* 1992, **75**, 59.

[14] U. Essmann, L. Perera, M. L. Berkowitz, T. Darden, H. Lee, L. G. Pedersen, *J. Chem. Phy.* 1995, **103**, 8577.

[15] H. Kim, Y. Kim, M. Yoon, S. Linn, S. M. Park, G. Seo, K. Kim, *J. Am. Chem. Soc.* 2010, **132**, 12200.